Proceedings of to the 9th Scientific Conference of University of Garmian:
Pure science and Technology Applications (SCUG-PSTA-2022).
Kalar (46021) / Sulaymaniyah (26-27 Oct.2022)
(Special issue for Passer journal of basic and applied sciences)
Paper No. 14, 205-219

Simulating the heat transfer behaviour in a fluidized bed by a combined thermal model in the CFD-DEM coupling

Sherko Ahmad Flamarz
Civil Engineering Department, University of Garmian, Kalar, Sulaymaniha
Kurdistan Government Region, Iraq
sherko.flamarz@garmian.edu.krd

ABSTRACT

The exchange of mass and heat transport in fluidized beds is a complicated and extensive topic, making it a rich field for scientific and industrial applications. This numerical research implements the CFD-DEM coupling to investigate the transport of heat energy in a fluidized bed. A numerical test compares the numerical and analytical results for a single particle in a column. Two cases of heating and cooling are compared. The numerical results present well adequacy with the analytical results. The development of fluidized bed units, within fluidized bed units is vital to improving the designs of these units. Therefore, three methods of column heating, including base heating, walls heating, and as well as walls and base heating, have been proposed in the simulations. The results reveal that the fluid inlet velocity increase during the fluidized beds' heating process is invalid. Thus, the fluid's proper inlet velocity and imposed temperature are crucial in the heating process for the fluidized beds since the particles need to provide time for the heat transport process.

KEYWORDS: Fluidized bed, simulation, two phase flow, heat transfer, CFD-DEM

1 INTRODUCTION

Heat transfer in fluidized beds is a complicated and extensive topic, making it a rich field for scientific and industrial applications. The heat transfer investigations in fluidized beds generally focused on three aspects: particle to fluid, fluid to the particle, and wall (cooling or heating) to particles and fluid heat transfer [1-3]. Understanding the mechanisms and methods of exchange of heat energy and mass transport in fluidized bed systems is essential in many applications in the industrial process. Typically, in the systems of agroindustry, food manufacturing processes, powders, combustion, metallurgy, drying, etc. [4, 5]. In the past and before the development of computers and soft-wares, experimental investigations were the only way to study packed and fluidized beds. Despite the advantages of these experiments, they could not predict and explain the complexity of the fluidization process. The development in computer soft and hard wares are assisted to use the computers in complex calculations tasks in modeling and simulations.

The coupling of CFD-DEM can distinguish the heat exchange between the solid phase particles and the fluid and solid phases. The first model of coupling CFD-DEM was developed by Tsuji et al. [6] to study the behavior of gas fluidized bed. Many studies are proposed the CFD-DEM coupling accompanied by heat transfer [2, 7-9]. Borkink and Westerterp [10] proposed a mechanism to describe heat transfer with a bed of particles. Malone and Xu. [11] are investigating the behavior of heat transfer in fluidized beds on the particle-scale flow level by proposing two convection models in liquid-solid fluidized beds. Stefan et al. [12] compared the numerical results of coupling CFD-DEM with empirical data for a fluidized bed heated by hot air. Chunhua Wang et al. [13] studied the spouted bed by CFD-DEM coupling in the particle cooling process. Other authors [14-20] proposed models of coupling CFD-DEM to investigate heat transport in gas-fluidized beds, pneumatic conveying units, etc.

The novelty of this work is proposing three methods for heating the column of fluidized beds and comparing the three methods to develop, improve, and economize energy consumption in fluidized bed reactors. In this work, a thermal model of heat transfer is integrated into the CFD-DEM coupling to investigate the heat transfer behaviors in a fluidized bed. Subsequently, the numerical implementation is validated by comparing the numerical results with the analytic results.

2. METHODS AND MATERIALS

2.1 FLUID PHASE: COMPUTATIONAL FLUID DYNAMICS (CFD)

The CFD code is based on the Reynolds-Averaged Navier-Stokes (RANS) equations to solve the incompressible flow (continuity and momentum equations) [21];

- Continuity equation:

$$\frac{\partial \rho_f}{\partial t} + \vec{\nabla} \cdot (\rho_f \vec{v}\ ) = 0 \tag{1}$$

- Momentum equation of the quantity of motion:

$$\frac{\partial \rho_f \vec{v}}{\partial t} + \vec{\nabla} \cdot (\vec{v} \times \vec{v}) = -\vec{\nabla} p + \vec{\nabla} \cdot \overset{=}{\tau} + \rho_f \vec{f} \tag{2}$$

Where t is time, ρ_f , and p are density, velocity, and pressure of the fluid respectively, $\overset{=}{\tau}$ is the viscous stress tensor and $\vec{f}$ refers to other body forces.

A hypothesis is needed to close Reynolds-Averaged Navier-Stokes (RANS) equations systems. The Boussinesq hypothesis a standard method employs to relate the Reynolds stresses to the mean velocity gradients [22]. The present research uses the standard k-ε model, largely used by practical engineering turbulence flow problems and calculations. The standard k-ε model is based on model transport equations for the turbulence kinetic energy (k) and its dissipation rate (ε) [23]; the equations are written as:

$$\rho_f \frac{\partial k}{\partial t} + \nabla \cdot \left(\rho_f \vec{v} k - (\mu + \frac{\mu_t}{\sigma_k}) \operatorname{grad} k \right) = P + G - \rho_f \varepsilon \tag{3}$$

$$\frac{\partial \varepsilon}{\partial t} + \nabla \cdot \left(\rho_f \vec{v} \varepsilon - (\mu + \frac{\mu_t}{\sigma_\varepsilon}) \operatorname{grad} \varepsilon \right) = C_{\varepsilon 1} \frac{\varepsilon}{k} \left[P + (1 - C_{\varepsilon 3}) G \right] P - \rho_f C_{\varepsilon 2} \frac{\varepsilon^2}{k} \tag{4}$$

$$v_t = \frac{\mu_t}{\rho_f} = C_\mu \frac{k^2}{\varepsilon} \tag{5}$$

where μ is viscosity, μ_t is turbulent viscosity, P accounts for the production of the kinetic energy through mean shear stresses, G is production term related to gravity effects and finally $\sigma_k = 1$, $\sigma_\varepsilon = 1.3$, $C_{\varepsilon 1} = 1.3$, $C_{\varepsilon 2} = 1.92$, $C_\mu = 0.09$, $C_{\varepsilon 3} = 0$ if $G \geq 0$ and $C_{\varepsilon 3} = 1$ if $G \leq 0$ are constants.

2.2 SOLID PHASE: DISCRETE ELEMENT METHOD (DEM)

The Discrete Element Method (DEM) is used to model the solid phase (particles); Cundall and Strack [24] developed the Discrete Element Method (DEM) model to study soil mechanics. The DEM model provides the location (coordinates), velocity, and contact force of each particle (solid phase) at each step. The motion of each particle is governed by Newton's second law of motion, and can be expressed, for the i-particle, by:

$$m_{i,p} \frac{d\vec{v}_{i,p}}{dt} = m_{i,p} \vec{g} + \sum_{j=1}^{nc} \vec{F}_{C,ij} + \vec{F}_{D,i,p} + \vec{F}_{B,i,p} \tag{6}$$

$$I_{i,p}\frac{d\vec{\omega}_{i,p}}{dt}=\vec{T}_{i,p} \quad , \quad I_{i,p}=\frac{2}{5}m_{i,p}r_{,pi}^{2} \tag{7}$$

where $\vec{v}_{i,p}$ is velocity of the (i th) particle, m_i is mass particle, $\vec{g}$ is gravity acceleration, n_c is number of contacts between the particles, $\vec{F}_{C,ij}$ is contact forces, $\vec{F}_{D,i,p}$ is drag force, $\vec{F}_{B,i,p}$ is buoyancy force. $I_{i,p}$ is moment of inertia, $\vec{\omega}_{i,p}$ is rotational velocity, $\vec{T}_{i,p}$ is torque and $r_{i,p}$ is radius.

The drag force ($\vec{F}_{D,i,p}$) represent the affect between the fluid phase (CFD) and solid phase (DEM) in other word the coupling of CFD-DEM. The drag force is expressed according to relation proposed by Helland et al. [25]:

$$\vec{F}_{D,i,p}=\frac{C_{D,i,p}}{8}\pi\rho_f d_{i,p}^{2}\left\|\vec{v}_f-\vec{v}_{i,p}\right\|\left(\vec{v}_f-\vec{v}_{i,p}\right)\varepsilon_f^{2} f\left(\varepsilon_f\right)^{m} \tag{8}$$

where $C_{D,i,p}$ is particle drag coefficient, $d_{i,p}$ is particle diameter, $\rho_f, \vec{v}_f, \varepsilon_f$ are density, velocity and local porosity of the fluid, and $m.n$ is a parameter. $f(\varepsilon_f)$ is porosity function [26]:

$$f(\varepsilon_f)=\varepsilon_f^{\,-n}, \quad and \quad f(\varepsilon_f)^{m}=\varepsilon_f^{\,-m.n} \tag{9}$$

The drag coefficient on a particle is function of Reynolds number ($\mathrm{Re}_{i,p}$), and $C_{D,i,p}$ is given [23]:

$$C_{D,i,p}=\begin{cases}\dfrac{24}{\mathrm{Re}_{p,i}}(1+0.15\,\mathrm{Re}_{p,i}^{0.687}) \text{ if } \mathrm{Re}_{i,p}<1000, & \mathrm{Re}_{i,p}=\dfrac{\varepsilon_f\rho_f d_{p,i}\left\|\vec{v}_f-\vec{v}_{p,i}\right\|}{\mu_f} \\ 0.44 \qquad\qquad \text{if } \mathrm{Re}_{i,p}\geq 1000 & \end{cases} \tag{10}$$

2.3 HEAT TRANSFER MODELLING (THERMAL APPROACH)

Modes of heat transfer in the solid phase (particles) in a fluidized bed are transported by conduction (contact between particle-particle and particle-wall), convection between the fluid phase and solid phase, and fluid phase and wall (cooling or heating). In this work, a combined thermal approach (conduction-convection) with the coupling of CFD-DEM is used to study the behavior of heat transfer in a fluidized bed, so:

$$mC_{p,i}\frac{dT_i}{dt}=\Phi_{ij,Conduction}+\Phi_{i,Convection} \tag{11}$$

where m is fluid mass, $C_{P,i}$ is heat capacity, $\Phi_{ij,Conduction}$ is heat transferred between the particles Ω_i and Ω_j , and $\Phi_{i,Convection}$ is heat transport by convection.

$$\Phi_{ij,Conduction} = H_{ij,C}(T_j - T_i), \quad and \quad H_{ij,C} = 2k_i a = 2k_i \left(\frac{3F_n a^*}{4E^*}\right)^{\frac{1}{3}} \tag{12}$$

where $H_{ij,C}$ is the contact conductance between the particles Ω_i and Ω_j with j varies from 1 to N (contact number), k_i is particle thermal conductivity, F_n is normal force, a is hertzian radius, a^* is equivalent radius , and E^* is an equivalent Young's modulus between the contacted particles.

$$\Phi_{i,Convection} = h_i S_i (T_s - T_\infty) \tag{13}$$

where h_i is heat transfer coefficient, T_s temperature of particle surface, T_∞ temperature of fluid and S_i is surface area of contact particle with the fluid [2].

Many of empirical and theoretical investigations are settled equations to calculate the value of heat transfer coefficient from the Nusselt number (Nu), where the Nusselt number is the ratio of convection heat transfer in the fluid in motion (through the Prandtl number $\Pr = \frac{C_{p_f} \cdot \mu_f}{k_f}$) to the conduction heat transfer in the flow regime (through the Reynolds number). The Nusselt number is founded from the set of equations proposed by Li & Mason [27] as followings:

$$Nu_{i,p} = \frac{h_{i,p} \ d_{i,p}}{k_f} = \begin{cases} 2 + 0{,}6\varepsilon_{i,p}^{m.n} \operatorname{Re}_{i,p}^{0{,}5} \Pr^{\frac{1}{3}} & \operatorname{Re}_{i,p} < 200 \\ 2 + \varepsilon_{i,p}^{m.n} (0{,}5 \operatorname{Re}_{i,p}^{0{,}5} + 0{,}02 \operatorname{Re}_{i,p}^{0{,}8}) \Pr^{\frac{1}{3}} & 200 < \operatorname{Re}_{i,p} < 1500 \\ 2 + 0{,}000045\varepsilon_{,i,p}^{m.n} \operatorname{Re}_{i,p}^{1{,}8} & \operatorname{Re}_{i,p} > 1500 \end{cases} \tag{14}$$

where k_f is fluid thermal conductivity, $\varepsilon_{i,p}$ is porosity of particle and $m.n$ equals 4.7. Then, substituting the equations 12 and 13 in equation 11 yields.

$$mC_{p,i} \frac{dT_i}{dt} = \sum_{j=1}^{N} H_{ij,C}(T_j - T_i) + h_i S_i (T_s - T_\infty) \tag{15}$$

Finally, the temperature of the particle Ω_i is calculated by integrating equation 14 into the Discrete element method (DEM) code, as follow:

$$T_i^{t+\Delta t} = T_i^t + \frac{\Delta t}{mC_{p,i}}\left[\left[\sum_{j=1}^{N} H_{ij,C}(T_j^t - T_i^t)\right] + h_i S(T_s - T_\infty)\right] \tag{16}$$

3. RESULTS AND DISCUSSIONS

The numerical approaches and modelling have been developed to investigate and simulate the difficult phenomena that accompanied the transport of heat and energy.

3.1 VALIDATION OF THERMAL APPROACH WITH THE ANALYTICAL CALCULATION

The integration of the thermal approach in the CFD–DEM coupling is tested. A single particle (sphere) in a column is tested numerically, comparing the numerical results with the analytical results. The comparison has been made for two cases (heating and cooling) between the temperatures of the sphere, which is calculated by the model with the analytical calculation from the equation below for pure convection:

$$T_p = T_f + \left[\left(T_{p,o} - T_f\right) EXP\left(\frac{-hS_p t}{mC_P}\right)\right] \tag{17}$$

where $T_{p,o}$ is initial temperature T_p is final temperature of the particle respectively, T_f is temperature of the fluid, S_p is the surface area of the particle, and t is the time.

A spherical particle is put in the center of a column (D = 51 mm, H = 0.75 m), under the effect of an upward flow of water, with a flow rate of 0.08 m/s. The physical properties of the aluminum particle and water are detailed in Table 1. For this test, two cases are checked: the heating and the cooling of the sphere. In the case of heating, the initial temperature of the particle and the fluid in the column is; 20 ^oC. The boundary condition for the heated surface is 80 ^oC. In the case of cooling, this temperature becomes; 80 ^oC, and the boundary temperature for the cooling surface becomes 20 ^oC.

The Comparison of the simulation and analytic results for the heating and cooling cases are depicted in Figure 1. The heating and cooling curves show that the numerical results present good adequacy with the analytical results. Thus, the proposed thermal model integrated into the CFD-DEM can deal with a natural and complex system in fluidization units.

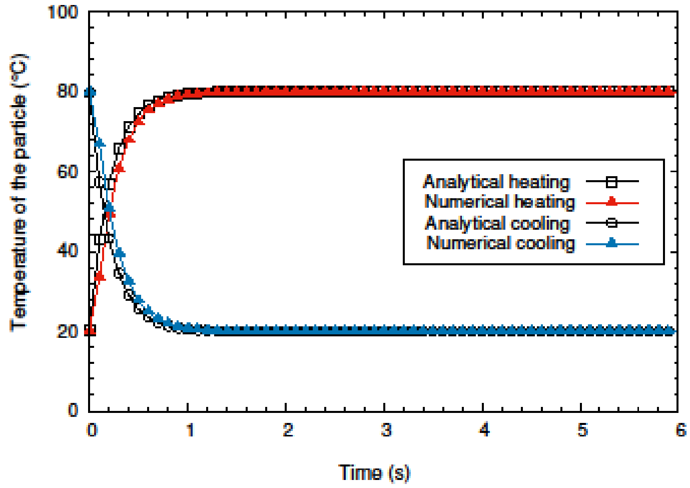

Figure 1: Temperature distribution for the heating and cooling cases.

Table 1. Physical properties and dimensions of simulated system.

Particle properties (Aluminium)		Fluid properties (Water)	
Particle diameter, d_p	1.5 mm	Viscosity, μ_f	0.001 kg/m.s
Density, ρ_p	2700 kg/m^3	Density, ρ_f	1000 kg/m^3
Heat capacity, C_p	900 J/kg.K	Heat capacity, C_f	4200 J/kg.K
Thermal conductivity, k_p	237 W/m.K	Thermal conductivity, k_f	0.6 W/m.K
Number of particles	2244	Bed height, H	75 cm
Young modulus, *E*	69 GPa	Bed width (diameter)	5.1 cm
Poisson ratio, ν	0.35	Bed thickness	0.15 cm
Friction coefficient, μ	0.4	Time step, Δt	5x10^{-6} sec

3.2 THERMAL MODELLING OF THE FLUIDIZATION PROCESS

The development of fluidized bed units, need to understand what goes on inter these processes within fluidized bed units is vital to improving designs for these units. For this, three methods of column heating have been proposed as following; a) heating the base (inlet), b) heating the walls, c) heating the base and the walls (see Figure 2). The system consist of spherical particles of Aluminium are placed in a column. The properties of the particles and water, and the dimensions of geometry are presented in Table 1. The height of the bed at rest (h = 9.9 cm) and the thickness of bed is one particle diameter (d_p=1.5 mm). The bed particles were fluidized over a range of inlet water velocities (0.08 m/s, 0.12 m/s and 0.16 m/s) for heating temperatures (boundary condition for the heating surface or the temperature impose) of 60 and 100 °C. The initial temperature for the particles and the inlet water were set at 20 °C.

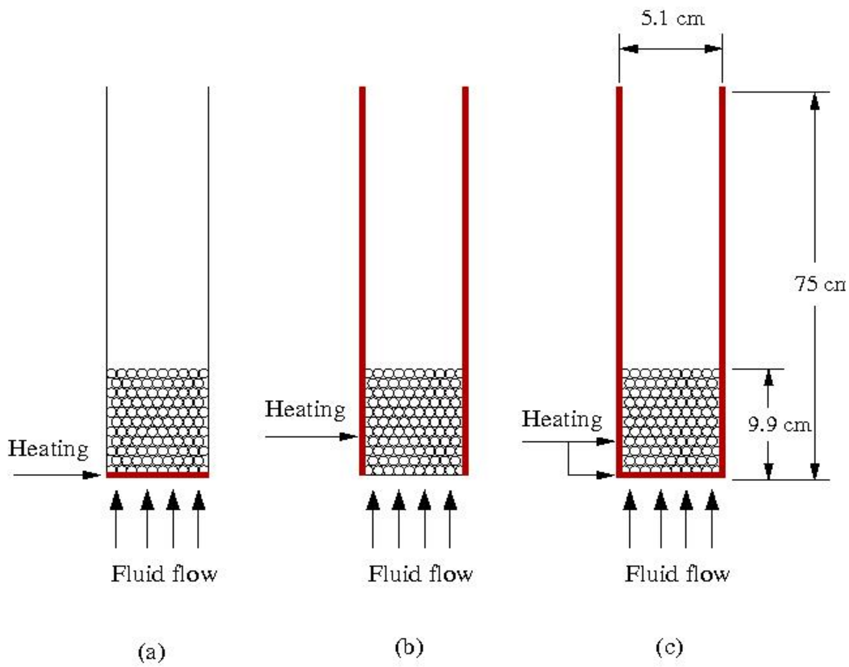

Figure 2: Sketch of three methods of column heating; a) base heating, b) wall heating, c) wall and base heating.

3.2.1. MEAN TEMPERATURE OF PARTICLE

The mean temperatures of particle are plotted as a function of simulation time as shown in Figures 3 and 4. They depict the mean temperature of particle with three different water fluidization velocities 0.08 m/s, 0.12 m/s, and 0.16 m/s, for three methods of heating with imposed temperatures (T_{impose} of 60 °C and 100 °C). The development of the temperature curves for base heating and base plus wall heating are increase with the time. They are reached steady state after 3 seconds from start of simulation, as depicted in Figure 3 and Figure 4. In other hand, the value of mean temperature for wall heating is not progress and still near the initial temperature, and the heating temperature not passing 5 ^oC (mean temperature didn't pass 25 ^oC).

This can be explained from the fact that the flow of water and particles are prevented the wall, whereas the stresses are concentrated and the collusions time of contact between the particles and heating walls is very short that is not sufficient for exchanging heat and energy. The results of heated wall method were consistency with the results of Malone, and Xu [11] . Thus, the two heating methods of base and base plus wall heating are more efficacious rather than the wall heating method in which the particles exchange the heat energy with the heating surfaces. From the Figures 3 , 4, for the two methods base column heating and base plus wall column heating are almost matching results and the temperature are developed until it has reached a steady state for the two case of heating surfaces with (T_{impose} = 60 °C and 100 °C).

In comparing between the two methods of heating; base column heating and base plus wall column heating, the first method will take the advantage, because it is less complex in terms of engineering in industrial applications and less costly for energy consumption.

The inlet velocity is essential in fluidization process; Figure 5 reveals a comparison between the results of the three inlet water fluidization velocities 0.08 m/s, 0.12 m/s and 0.16 m/s of solid phase (particles) heating process. The Figure 5 a, b reveals the mean particle temperature of base column heating for first four seconds from the start of simulation of fluidization process. It is obvious that the water velocity (v_f = 0.12 m/s) is fully fluidized the bed and reaches the thermal steady state before two others water velocities 0.08 m/s and 0.16 m/s (see Figure 5 a, b).

The results in Figure 5 reveals that the increase of inlet velocity of the fluid in heating process in fluidized beds it doesn't have to be useful. In fact, the high velocity of the fluid didn’t give the time to transport of heat and energy between particle–particle, particle–heating surface and particle–fluid. In other hand, the low velocity of the fluid in heating process may cause overheating to the particles. Thus, the proper inlet velocity of fluid and imposed temperature is crucial in heating or cooling process in fluidized beds.

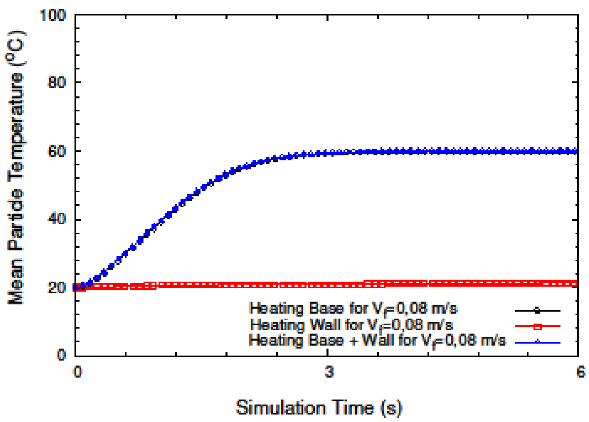

(a)

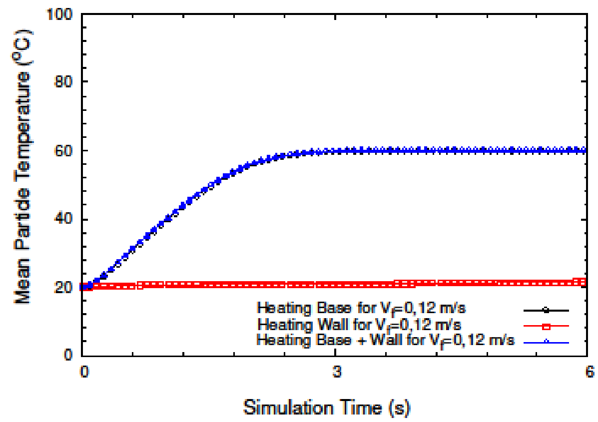

(b)

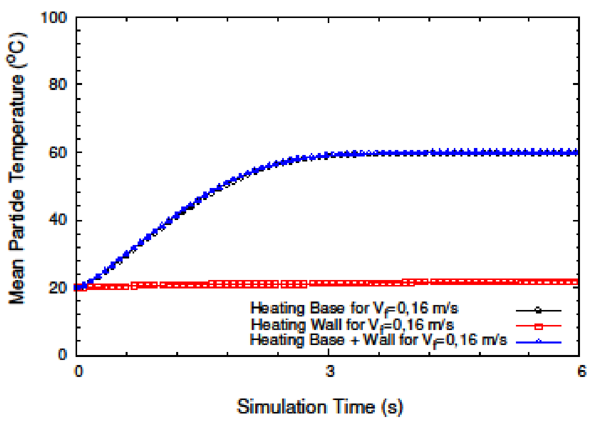

(c)

Figure 3: Mean temperature distribution of particle for: a) Base heating, b) Wall heating, c) Wall and base heating. (T_{impose}=60 °C).

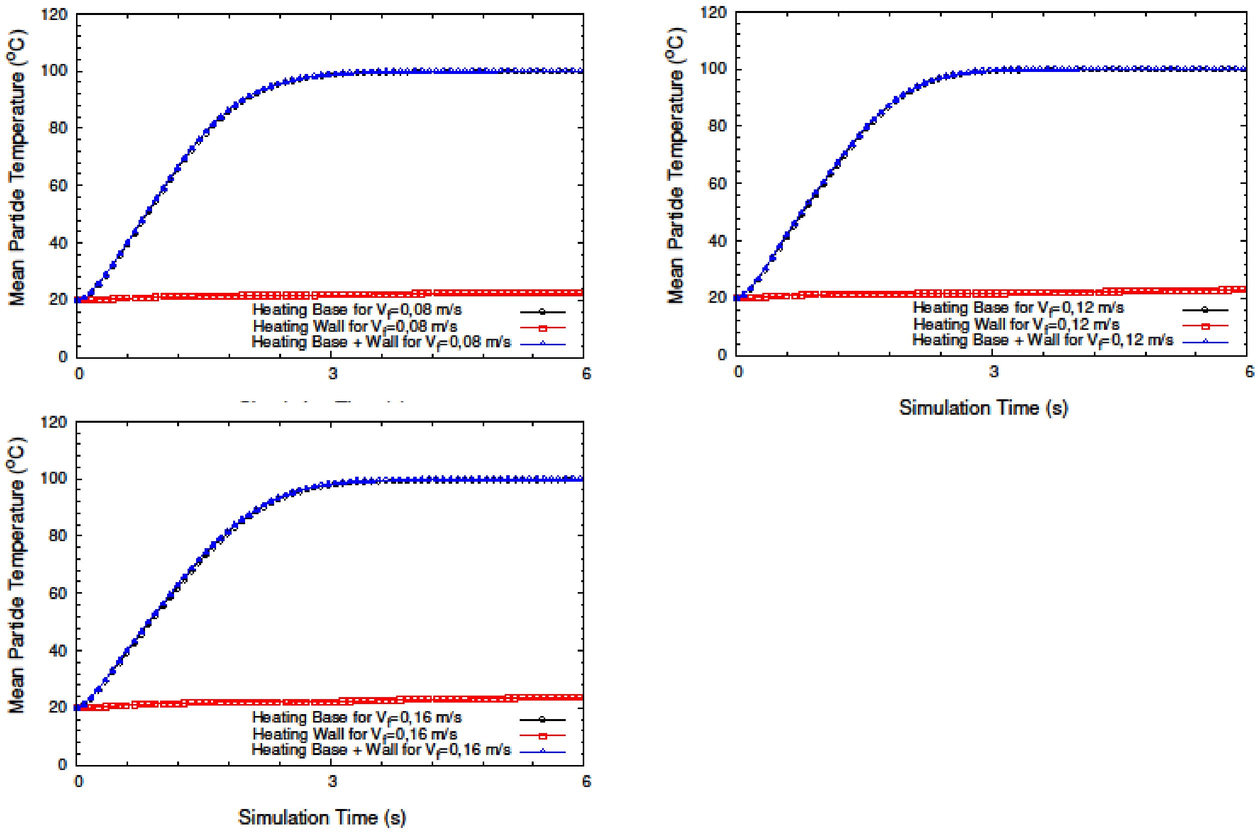

(c)

Figure 4: Mean temperature distribution of particle for: a) Base heating, b) Wall heating, c) Wall and base heating. (T_{impose}=100 °C).

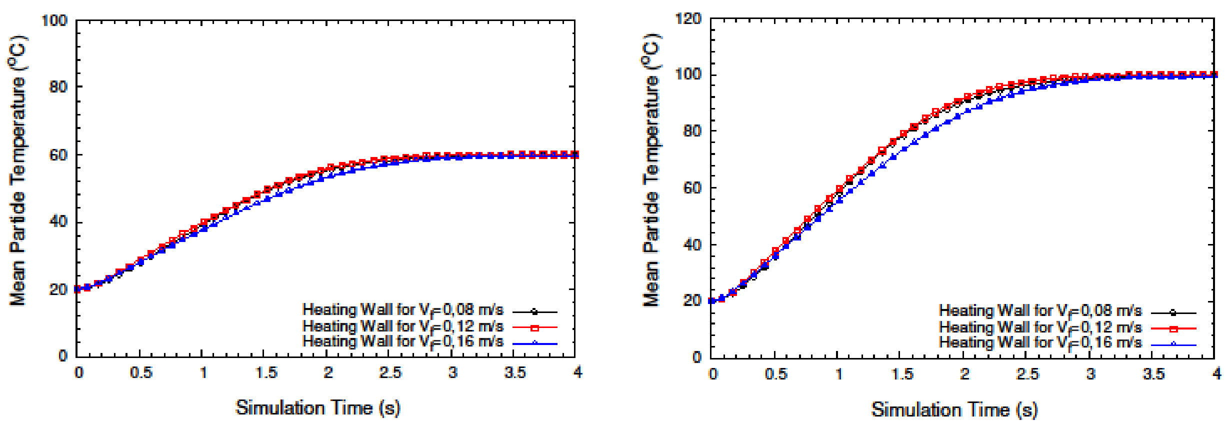

(a) **(b)**

Figure 5: Mean temperature distribution of particle for: a) heating base for T_{impose} = 60 °C, b) heating base for T_{impose} = 100 °C.

Figure 6 a-g, is depicted the snapshots of temperature development as a function of time in the fluidized of base heated method for inlet water velocity v_f=012 m/s and the base heated to 100 ^oC (T_{impose} = 100^oC). The snapshots (a-d) in Figure 6, shows the starting of the fluidization under the effect of drag force, when water passes through the interstitial clearance between the particles upward from the bottom of the column, the drag force between the water and the static bed trend the bed (particles) to move upward. The drag force will push the bed to overcome the gravity force of particles. After about the three seconds the fluidized bed (particles) trend to be uniform and stable. The good mixing of the particles with the water, increase the contact between the solid phase (particle-particle), solid phase with the walls (particle-heated surface and walls), the particles with the water, and fluid phase with the heated surfaces are developed the heat exchange between the two phases as shown in Figure 6 e-g, (the temperature profile is in Kelvin). The Figure 6 reveals the well integration of the thermal model with the CFD-DEM coupling.

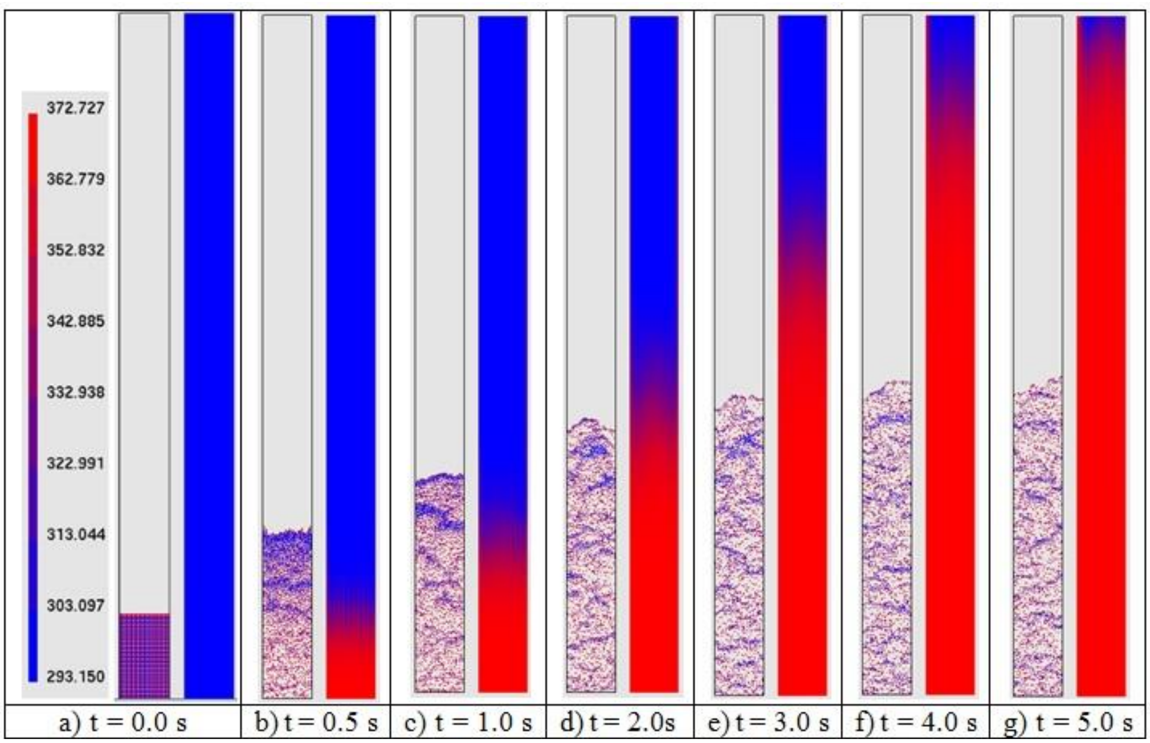

Figure 6: Snapshots of temperature development in the fluidized bed. v_f = 0.12 m/s and T_{impose} = 100^oC.

4. CONCLUSIONS

This study investigates the heat transfer behavior in a fluidized bed by implementing a thermal model of conduction-convection with CFD-DEM coupling. The thermal approach considers almost all the known mechanisms of heat transfer, including conduction between particle-particle and pipe wall–particle, as well as convection between particle–fluid, pipe wall–particle, fluid–pipe wall, and fluid with the heated surfaces. All these mechanisms are applied in this study. A numerical validation has been done for the thermal approach, comparing the simulation and analytic results for the heating and cooling cases for a single particle in a column. The numerical results present excellent adequacy with the analytical results. Then, three methods of column heating have been proposed as follows, heating the base (inlet), heating the walls, and heating the base and the walls have been proposed in the simulations. The development of the temperature curves for base heating and base plus wall heating increases with time. They reached a steady state after 3 seconds from the start of the simulation. On the other hand, the mean temperature value for wall heating is not progress and is still near the initial temperature, and the heating temperature does not pass 5 ^{o}C. The simulations results show that the method of the heating wall was not reached the thermal steady state, which can be explained by the fact that the flow of water and particles prevented the wall, where stresses are concentrated, and the collusions time of contact between the particles and heating walls is a short time. It is not sufficient for heat and energy exchange to occur. The results of the heated wall method were consistent with the results of Malone and Xu [11]. The results reveal that; the increase of inlet velocity of the fluid in the heating fluidized beds process was not helpful. The high velocity of the fluid did not give the time to transport heat and energy between particle-particle, particle–heating surface, and particle–fluid. Thus, the proper inlet velocity of the fluid and imposed temperature is crucial in the heating process in fluidized beds since the particles need to provide time for the heat transport process.

5. REFERENCES

1. Azmir J., Q. Hou, A. Yu, Discrete particle simulation of food grain drying in a fluidised bed. Powder Technology, 2018. **323**: p. 238-249.
2. Al-Arkawazi, S., C. Marie, and P. Coorevits, Modeling the heat transfer between fluid-granular medium. Applied Thermal Engineering, 2018. **128**: p. 696-705.

3. Nguyen V.D., C. Cogné, M. Guessasma, E. Bellenger, J. Fortin, Discrete modeling of granular flow with thermal transfer: Application to the discharge of silos. Applied Thermal Engineering, 2009. **29**: p. 1846-1853.

4. Chaudhuri B., F. J. Muzzio, and M. S. Tomassone, Modeling of heat transfer in granular flow in rotating vessels. Chemical Engineering Science, 2006. **61**: p. 6348-6360.

5. Miao H., H. Zhang, X. An, J. Chen, and A. Yu, Combined effects of particle shape, incident angle and porosity on momentum and heat transfer between spheroids and fluids. International Journal of Heat and Mass Transfer, 2022. **197**: p. 123341.

6. Tsuji, Y., T. Kawaguchi, and T. Tanaka, Discrete particle simulation of two-dimensional fluidized bed. Powder Technology, 1993. **77**: p.79-87.

7. Simsek E., B. Brosch, S. Wirtz, V. Scherer, and F. Krüll, Numerical simulation of grate firing systems using a coupled CFD/discrete element method (DEM). Powder Technology, 2009. **193**: p. 266-273.

8. Patil A.V.l, E.A.J.F. Peters, and J.A.M. Kuipers, Comparison of CFD-DEM heat transfer simulations with infrared/visual measurements. Chemical Engineering Journal, 2015. **277**: p. 388-401.

9. Tsory T., N. B. Jacob, T. Brosh, and A. Levy, Thermal DEM–CFD modeling and simulation of heat transfer through packed bed. Powder Technology, 2013. 244: p. 52-60.

10. Borkink J. G. H., and K. R. Westerterp, Influence of tube and particle diameter on heat-transport inpacked-beds. A.I.Ch.E.Journal, 1992. 38: p. 703.

11. Malone, F., and B.H. Xu, Particle-scale simulation of heat transfer in liquid-fluidized beds. Powder Technology, 2008. 184: p. 189-204.

12. Rickelt S., F. Sudbrock, S. Wirtz, and V. Scherer. Coupled dem/cfd simulation of heat transfer in a generic grate system agitated by bars. Powder Technology, 2013. 249: p. 360–372.

13. Wang C., Z. Zhong, X. Wang, and Siti Aisyah Alting, Numerical Simulation of Gas-Solid Heat Transfer Behaviour in Rectangular Spouted Bed. The Canadian Journal of Chemical Engineering, 2015. 93, p. 2077-2083.

14. Jun D. , G M Hu, Z. Q. Fang, W. Gui, Simulation of dilute pneumatic conveying with bends by CFD-DEM. International Journal of Fluid Machinery and Systems, 2015. 8(2), p. 84-93.

15. Tsory T., N. B. Jacob, T. Brosh, and A. Levy, Thermal DEM-CFD modelling and simulation of heat transfer through packed bed. Powder Technology, 2013. 244, p. 52–60.

16. Sherko Ahmad Flamarz, Computational Study of Heat Transfer Behavior in Fluid-Solid Fluidized Beds, Sulaimani Journal for Engineering Sciences, 2020. 7: p. 25-41.

17. Brosh T., and A. Levy, Modeling of Heat Transfer in Pneumatic Conveyer Using a Combined DEM-CFD Numerical Code', Drying Technology, 2010. 28(2): p. 155-164.

18. Zhuang Y.Q., X.M. Chen, Z.H. Luo, and J. Xiao, CFD-DEM modeling of gas-solid flow and catalytic MTO reaction in a fluidized bed reactor. Computers and Chemical Engineering, 2014. 60: 1-16.

19. Chu K., Y. Chen, L.Ji, Z. Zhou, A.Yu, and J. Chen, Coarse-grained CFD-DEM study of Gas-solid flow in gas cyclone, Chemical Engineering Science, 2022. 260, 12.

20. Zhu G., Y. Zhao, Z. Wang, M. S. Khalid , and M. Liu, Semi-resolved CFD-DEM simulation of fine particle migration with heat transfer in heterogeneous porous media. International Journal of Heat and Mass Transfer, 2022. 197, 123349.

21. Archambeau F., N. Méchitoua, and M. Sakiz, Code_Saturne: a finite volume method for the computation of turbulent incompressible flows–industrial applications, Int. J. Finite Volumes, 2004. 1: p. 1–62.

22. Launder B.E., and D.B. Spalding, The numerical computation of turbulent flows. Comput. Meth. Appl. Mech. Eng., 1974. 3: p. 269-289.

23. Schiller L., and A.Z. Naumann, A drag coefficient correlation. Ver. Deut. Ing., 1935. 77: p. 318-320.

24. Cundall P.A, and O.D.L. Strack, A discrete numerical model for granular assemblies. Geotechnique, 1979. 29: p. 47-65

25. Helland, E., R. Occelli, and L. Tadrist, Computational study of fluctuating motions and cluster structures in gas-particle flows. International Journal of Multiphase Flow, 2002. 28: p. 199-223.

26. Mukherjee A.K., and B.K. Mishra, Experimental and simulation studies on the role of fluid velocity during particle separation in a liquid–solid fluidized bed. Int. J. Miner. Process. 2007. 82: p. 211-221.

27. Li, J., and D. Mason, Simulation of gas-solids flow in pipes with heat transfer using the distinct element method. Chemical Engineering Research Event, paper 71, Institution of Chemical Engineers, Rugby, UK, 1998.